Stray Load Loss Analysis of Canned Induction Motor for Hermetic Compressor

Katsumi Yamazaki* and Yoshihisa Haruishi**

Abstract - In this paper, we investigate the main components of stray load loss of induction motors for ammonia compressors. The variations of the losses at each part of the motor due to load are calculated by the combined 3-D-2D finite element method formulated by the mixed moving coordinate systems. The stray load loss is calculated from these results due the definition of IEEE standard-112. It is clarified that the core loss and the eddy current loss of the can increase due to load, which can be considered as the main part of the stray load loss.

Keywords: Induction motor, iron loss, stray load loss, finite element method, combined 3D-2D analysis.

1. Introduction

Owing to the regulation of Freon gas in environmental problem, ammonia is recently revalued as refrigerant of compressors. Accordingly, the canned motors are developed as reliable drivers of hermetic type ammonia compressors. Fig. 1 shows the outline of the motor. The motor has a thin, cylindrical, metallic can inserted in air gap of a cage induction motor to prevent ammonia from entering the stator and damaging the primary windings. The can is fixed on the stator. Both the motor and the compressor are enclosed in the container.

On the other hand, the efficiency of the motor may decrease because of the eddy current loss in the can. Furthermore, the air-gap must be wide compared with usual induction motors in order to insert the can. This also causes the decrease of the efficiency of the motor. Therefore, it is an important subject to understand the characteristics of the losses for the design of the canned motors.

The electrical losses of the cage induction motors can be classified as:

(a) Primary copper loss: the Joule loss of the primary winding

(b) Secondary copper loss: the Joule loss of the rotor cage

(c) Iron loss: the eddy current and the hysteresis losses of the stator and the rotor cores.

(d) Stray load loss: the electrical losses except for (a)-(c).

However, when these losses are separated from the results of the measurement of the motor, it can be said that the obtained losses do not always satisfy the above relations. For example, the iron loss is obtained by the subtraction of the mechanical and the primary copper losses from the total no-load loss. Thus the iron loss obtained by the measurement includes other losses. Furthermore, the specification of the stray load loss is much complex. The losses of the core and the rotor cage often vary nonlinearly due to the load condition because of the magnetic saturation and the harmonic fields. As a result, the difference between the practical losses and the estimated losses is classified as the stray load loss [1].

In this paper, we calculate the losses at each part of the canned motor directly by the electromagnetic field analysis in order to understand the variation due to the load condition. The relationships between the calculated losses and the separated losses by the measurement are also discussed.

In the analysis of the canned motor, there are two problems. One is the large calculation time for the nonlinear time domain analysis with the consideration of the end-effects. The other is that the motor has the can and rotor cage, which are the conductors with relative velocity. When we select the fixed stator coordinate system for the analysis, the velocity term, which causes the oscillation of the solution [2], should be needed in the equation of the rotor cage [3]. On the other hand, in case of the moving rotor coordinate system, the velocity term should be needed in the can.

From these points of view, we apply the formulation of the mixed moving coordinate systems [4] to this motor. In the formulation, the governing equations of the stator and rotor regions are introduced by the fixed and moving coordinate systems, respectively. The regions formulated by the different coordinate systems are connected at the air-gap. In addition, to consider the end effect with the practical

* Department of Electrical Engineering, Chiba Institute of Technology, 2-17-1 Tudanuma, Narashino, Chiba 275-0016, Japan. (yamazaki@pf.it-chiba.ac.jp)

Received June 7, 2005 ; Accepted August 23, 2005

computer resources, the combined 3D-2D (three dimensional-two dimensional) finite element analysis [5] is applied. In the analysis, 3D frequency domain analysis is applied only to estimate the end-effects of the motor. The 2D nonlinear time domain analysis is carried out to calculate the losses of the motor with the result of the 3D analysis.

2. Calculation Method

2.1 Formulation of mixed moving coordinate systems

The general governing equations of the conductor whose velocity is V relative to the stator are [3]:

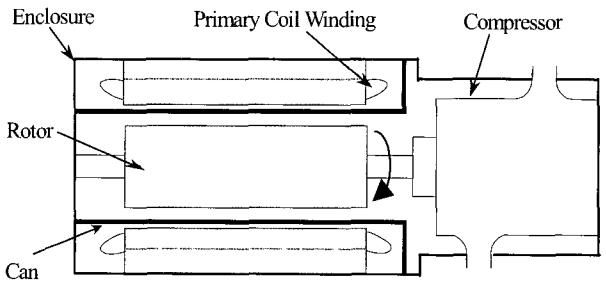

Fig. 1 Outline of canned motor

$$\nabla\times(\nu\nabla\times\mathbf{A})=\sigma\left\{-\frac{\partial\mathbf{A}}{\partial t}-\nabla\phi+(\mathbf{V}-\mathbf{V}_f)\times\nabla\times\mathbf{A}\right\} \tag{1}$$

$$\nabla\cdot\left\{\sigma(-\frac{\partial\mathbf{A}}{\partial t}-\nabla\phi+(\mathbf{V}-\mathbf{V}_f)\times\nabla\times\mathbf{A})\right\}=0 \tag{2}$$

where V_f is the velocity of the coordinate system relative to the stator, A and ϕ are the magnetic vector and the electric scalar potentials, ν is the reluctivity and σ is the conductivity of the conductor.

In this paper, we set $V_f=0$ at the stator region including the can and $V_f=V$ at the rotor region including the rotor cage whose velocity is V. In this case, the velocity term is vanished in all regions. On the other hand, in general, the definitions of the electromagnetic potentials introduced in the stator and rotor coordinate system are different [3]. They become identical when the proper gauge condition [4] is applied to the formulation, that is,

$$\mathbf{A}\cdot\mathbf{V}=0 \tag{3}$$

If the 2D analysis is utilized, this condition is satisfied automatically because the magnetic vector potential has only axial component that is right angle to V. In case of the 3D analysis, this condition can be imposed by the tree technique of the edge finite elements [6].

2.2 Combined 3D-2D finite element method

In the combined 3D-2D finite element analysis, the end effects of the motor is estimated by the frequency domain analysis, whose equations are derived from (1), (2) as

$$\nabla\times(\nu\nabla\times\mathbf{A})=\mathbf{J}_1+\sigma(-js\omega\mathbf{A}-\nabla\phi) \tag{4}$$

$$\nabla\cdot\{\sigma(-js\omega\mathbf{A}-\nabla\phi)\}=0 \tag{5}$$

where J_1 is current density of the primary coil, ω is the angular frequency of the power supply, s is the slip of the conductor. In the can region, s=1. The gauge condition (3) is also imposed. In this case, $js\omega A$ and $\nabla\phi$ in the equations have special meanings. As the peripheral component of A is set as zero by (3), the electric field of this direction is given only by $\nabla\phi$. On the other hand, the axial component of A is related to the magnetic vector potential used in the 2D formulation. Utilizing this property, we can obtain the coefficient, which modify the conductivity applied in the 2D analysis for the consideration of the end effects of the eddy current [7], that is,

$$k=\left|\frac{\int_S\int_A^B\nabla\phi\cdot dl dS}{\int_S\int_A^B js\omega\mathbf{A}\cdot dl dS}\right| \tag{6}$$

where A, B are points at the ends of the core length, S is the cross section of the conductor. The coefficient k corresponds to the ratio of the voltage drop of the peripheral direction to the total induced voltage.

Using the coefficient of (6), we can modify the 2D nonlinear time domain formulation as follows:

$$-\nabla(\nu\nabla)A_z = J_{1z}-(1-k)\sigma\frac{\partial A_z}{\partial t} \tag{7}$$

Following primary voltage equation is coupled to (7) in case of voltage input analysis.

$$V_{1m}=\frac{2ABN_1}{S_m}\frac{d}{dt}\int_{Sm}A_z\,dS+L_e\frac{dI_{1m}}{dt}+RI_{1m} \tag{8}$$

where V_{1m} is the primary voltage of m-th phase, N_1 is the number of turns of the primary coil, R is the primary coil resistance and L_e is the coil-end leakage inductance, which can be also obtained by the 3D frequency domain analysis.

2.3 Loss calculation

From the result of the combined 3D-2D finite element

analysis, the total Joule losses of the primary winding and rotor cage W_1, W_2 can be calculated as follows:

$$W_1 = \frac{1}{T}\int_0^T \left(\sum_{m=1}^{3} R I_{1m}^{\ 2} \right) dt \tag{9}$$

$$W_2 = \frac{1}{T}\int_0^T \int_{conductor} (1-k)\sigma \left| \frac{\partial A_z}{\partial t} \right|^2 dv dt \tag{10}$$

where T is the time period. On the other hand, the core loss W_c, which is the sum of the eddy current loss W_e and hysteresis loss W_h of the core, can be calculated from the time variation of the flux density as follows:

$$W_e = \frac{K_e D}{2\pi^2}\int_{iron} \frac{1}{N}\sum_{k=1}^{N} \left\{ \left(\frac{B_r^{k+1} - B_r^k}{\Delta t} \right)^2 + \left(\frac{B_\theta^{k+1} - B_\theta^k}{\Delta t} \right)^2 \right\} dv \tag{11}$$

$$W_h = \frac{K_h D}{T}\sum_{i=1}^{NE} \frac{\Delta V^i}{2} \left(\sum_{j=1}^{Npr^i} \left(B_{mr}^{ij} \right)^2 + \sum_{j=1}^{Np\theta^i} \left(B_{m\theta}^{ij} \right)^2 \right) \tag{12}$$

where D is the density of the core, N is the number of time steps per one time period, Δt is the time interval, ΔV_i is the volume of i-th finite element, B_r and B_θ are the radial and peripheral component of the flux density, $B_{mr}^{\ ij}$ and $B_{m\theta}^{\ ij}$ are the amplitude of each hysteresis loop. K_e and K_h are the experimental constant obtained by Epstein frame [8].

In addition, the eddy current loss of the can W_{can} is also calculated by the same expression of (10). As we will discuss in Section III, W_{can} is regarded as the part of the iron loss W_i.

$$W_i = (W_e + W_h + W_{can}) \tag{13}$$

3. Definition of Stray Load Loss

In the IEEE standard 112 method B, the stray load loss W_s is defined from the measured characteristics as

$$W_s = W_{Load} - W_{iNoload} - W_1 - W_{2Fundamental} - W_m \tag{14}$$

where W_{Load} is the total loss at the load condition, $W_{iNoload}$ is the iron loss at no-load condition, W_1 is the primary copper loss, $W_{2Fundamental}$ is the secondary copper loss determined by the fundamental component of the secondary current and the W_m is the mechanical loss.

Let us discuss the details of the right hand members in (14). The total loss at the load condition W_{Load} is obtained by the subtraction of the output power P_{out} measured by the dynamometer from the input power P_{in} as follows:

$$W_{Load} = P_{in} - P_{out} \tag{15}$$

The iron loss $W_{iNoload}$ is obtained from the losses at no-load condition, that is, the subtraction of the mechanical loss W_m and the primary copper loss $W_{1Noload}$ from the total no-load loss W_{Noload}.

$$W_{iNoload} = W_{Noload} - W_{1Noload} - W_m \tag{16}$$

Thus $W_{iNoload}$ in (14) can be considered as the losses generated at not only the core but also the other parts at no-load condition, such as the eddy current loss of the can.

On the other hand, the secondary copper loss $W_{2Fundamental}$ is defined with the slip s and the secondary input as follows:

$$W_{2Fundamental} = s(P_{in} - W_1 - W_{iNoload}) \tag{17}$$

Thus $W_{2Fundamental}$ in (14) can be regarded as the fundamental Joule loss of the rotor cage except for the harmonics.

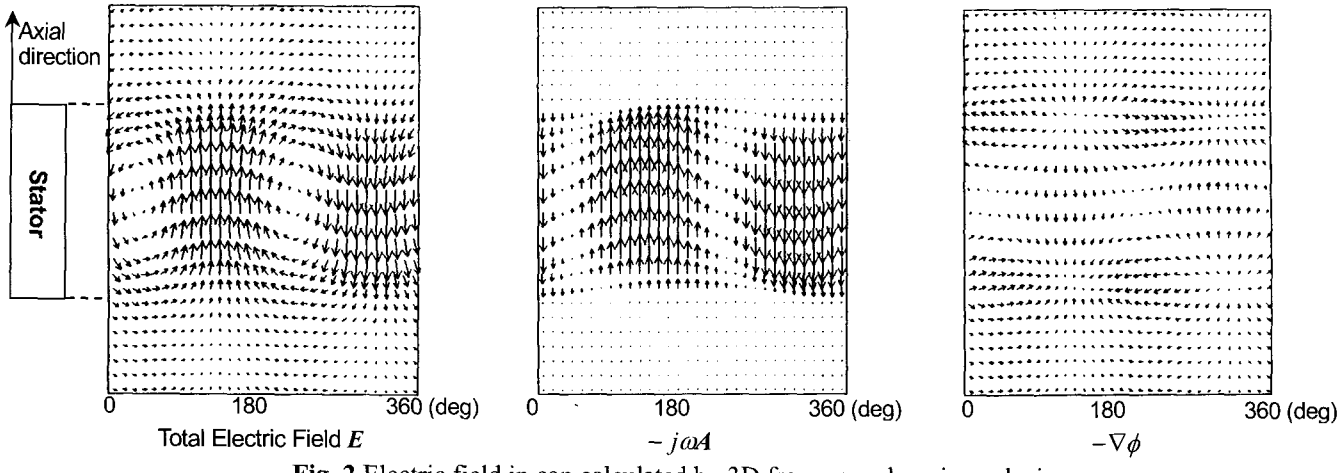

Fig. 2 Electric field in can calculated by 3D frequency domain analysis

On the other hand, as we discussed in Chapter II, the electromagnetic field analysis gives the total loss at load condition W_{Load} directly with the consideration of the harmonics as:

$$W_{Load} = W_1 + W_2 + W_i + W_m \tag{18}$$

Substituting (18) into (14), we have,

$$W_s = (W_2 - W_{2Fundamental}) + (W_i - W_{iNoload}) \tag{19}$$

Consequently, in this case, the stray load loss can be calculated from the difference between the total and fundamental Joule losses of the rotor cage and the difference between the iron losses at no-load and the load condition. In case of the canned motor, the iron loss W_i is regarded as the sum of the core loss and the eddy current loss of the can.

4. Results and Discussions

The analyzed motor is 150kW class 2-pole aluminum cage induction motor with 0.3mm can inserted in the air-gap.

Fig.2 shows the distributions of total electric field $\boldsymbol{E}$, $j\omega\boldsymbol{A}$ and $\nabla\phi$ in the can obtained by the 3D frequency domain finite element method with the gauge condition (3). It indicates that the peripheral component of the electric field is given only by $\nabla\phi$ because the peripheral component of $\boldsymbol{A}$ is set as zero. From this distribution, the modified coefficient of the conductivity of the can 1-k_{can} for the 2D analysis is calculated as 0.725. The modified coefficient of the rotor cage 1-k_{cage} is also obtained as 0.650 by the same analysis.

Fig. 3 shows the core loss distribution and time variation of flux density at no-load and rated load condition. In case of the no-load condition, the flux density waveform at the stator is nearly sinusoidal. On the other hand, the flux density at the rotor is nearly DC field because the slip is zero. On the contrary, when the motor is loaded, the flux density waveform of both the stator and the rotor include much time harmonics. This is mainly caused by the magnetic saturation at the bridge parts (top of the bars) of the rotor and the can due to the increase of the secondary currents. As a result, the core loss density much increases compared with the density at no-load condition. In expression (14), the core loss is assumed as constant due to the load condition because the iron loss at the load condition cannot be obtained by the measurement.

Fig.4 shows the calculated total losses in cases of the no-load and the rated load condition. The results of the losses before insertion of the can are also indicated. They indicate that the eddy current loss of the can is the largest loss and

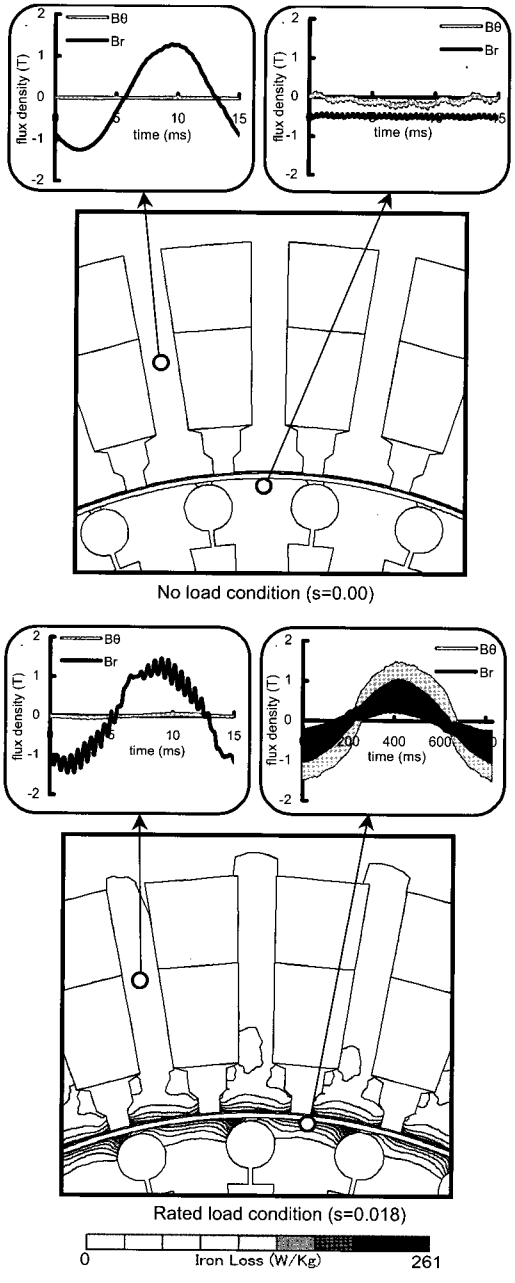

Fig. 3 Core loss distribution and time variation of flux density

that not only the primary and secondary copper losses but also the core and the can losses increase due to the load. These increase of the losses are classified as the stray load loss. The stray load loss calculated due to (19) is 6.4kW (4.3% of the output) in case of the canned motor and 2.3kW (1.5% of the output) in case of the motor without the can. In the IEEE standard, the average stray load loss of 150kW induction motors is regarded as 1.5%. The calculated result is reasonable. It can be said that both the no-load loss and stray load loss increase due to the insertion of the can.

Fig.5 shows the experimental and calculated efficiency of the motor. The experimental and calculated results agree well.

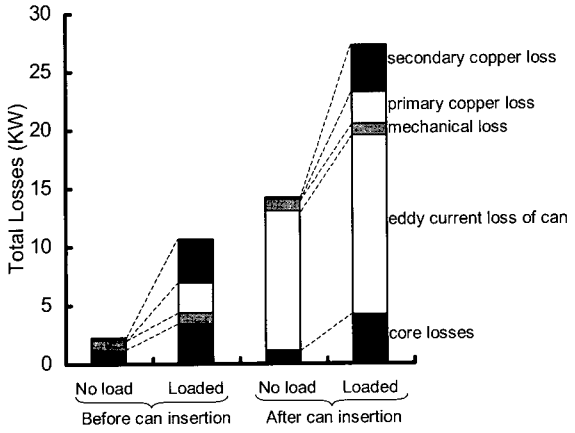

Fig. 4 Calculated total loss in each case

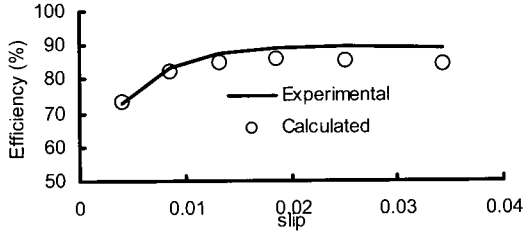

Fig. 5 Experimental and calculated efficiency

5. Conclusions

The losses including stray load loss of the canned motor are analyzed by the combined 3D-2D finite element analysis formulated by the mixed coordinate systems. It is clarified that the core losses and the eddy current loss of the can increase due to the load because of the increase of harmonic fields in the motor. The largest loss of the motor is the eddy current loss of the can. It can be said that both the no-load loss and the stray load loss increase due to the insertion of the can.

References

[1] K. Yamazaki and Y. Haruishi, "Stray load loss analysis of induction motor-Comparison of measurement due to IEEE standard 112 and direct calculation by finite element method," *IEEE Trans. Industry Applications.*, vol.40, no.2, pp.543-549, 2004.

[2] T. J. R. Hughes, "A Simple scheme of developing upwind finite elements," Int. J. Num. Mesh. Engng., vol.12, pp. 1359-1365 (1978).

[3] K. Yamazaki, "Generalization of 3D Eddy Current Analysis for Moving Conductors Due to Coordinate Systems and Gauge Conditions," *IEEE Trans. Magn.*, vol. 33, no.2, pp.1259-1262, 1997.

[4] K. Yamazaki, "3D Eddy Current Formulation for Moving Conductors with Variable Velocity of Coordinate System Using Edge Finite Elements," *IEEE Trans. Magn.*, vol. 35, no.3, pp.1594-1597, 1999.

[5] K. Yamazaki, "Induction Motor Analysis Considering both Harmonics and End Effects Using Combination of 2D and 3D Finite Element Method," *IEEE Trans. Energy Conversion*, vol.14, no.3, pp.698-703, 1999.

[6] R. Albanese and G. Rubinacci, "Solution of 3D eddy current problems by integral and differential methods," *IEEE Trans. Magn.*, vol. 28, pp.1228-1231, 1992.

[7] K. Yamazaki, "Modification of 2D Nonlinear Time-Stepping Analysis by Limited 3D Analysis for Induction Machines," *IEEE Trans. Magn.*, vol.33, pp.1694-1697, 1997.

[8] H. Domeki, Y. Ishihara, C. Kaido, Y. Kawase, S. Kitamura, T. Shimomura, N. Takahashi, T. Yamada and K. Yamazaki, "Investigaiton of benchmark model for estimating iron loss in rotating machine" *IEEE Trans. Magn.*, vol. 40, no.2, pp.794-797, 2004.